



AIAA 2002-0675

**Aircraft Icing Environments Observed
In Mixed-Phase Clouds**

Stewart G. Cober and George A. Isaac
Cloud Physics Research Division
Meteorological Service of Canada
Downsview, Ontario, Canada

40th Aerospace Sciences Meeting & Exhibit
14-17 January 2002
Reno, Nevada

For permission to copy or to republish, contact the copyright owner named on the first page.
For AIAA-held copyright, write to AIAA Permissions Department,
1801 Alexander Bell Drive, Suite 500, Reston, VA, 20191-4344.

AIRCRAFT ICING ENVIRONMENTS OBSERVED IN MIXED-PHASE CLOUDS

Stewart G. Cober and George A. Isaac

Cloud Physics Research Division, Meteorological Service of Canada, Downsview, Ontario, Canada

ABSTRACT

Aircraft icing environments in winter stratiform mixed-phase clouds are characterized and compared to similar characterizations for liquid-phase clouds. The characterization includes an analysis of the frequencies of occurrence of the liquid, ice and total water contents, determination of the average droplet and ice crystal spectra, and analysis of the liquid and ice water fractions. The analysis is based on data collected during 81 research flights conducted during the Canadian Freezing Drizzle Experiments, the Alliance Icing Research Study and the FIRE Arctic Cloud Experiment. The icing environments were assessed over horizontal extents of 3 km, in terms of liquid water content (LWC) and droplet median volume diameter (MVD). Overall, liquid, mixed and glaciated-phase cloud conditions were observed for 35%, 43% and 22%, respectively of the in-cloud observations with temperatures $\leq 0^{\circ}\text{C}$.

It is shown that the characteristics of mixed-phase icing environments can be substantially different from those in liquid-phase environments. Specifically, mixed-phase icing environments with potential accumulations $> 6 \text{ g cm}^{-2} \text{ h}^{-1}$ were never observed for supercooled large drop (SLD) conditions with droplet MVD $> 70 \mu\text{m}$. However, 14% of the liquid-phase icing conditions with $> 6 \text{ g cm}^{-2} \text{ h}^{-1}$ had MVD $> 70 \mu\text{m}$. Similarly, while mixed-phase conditions were observed for 43% of the overall in-cloud measurements, less than 20% of the in-cloud cases with MVD $> 50 \mu\text{m}$ were assessed as being mixed-phase. It is suggested that the co-existence of SLD and ice crystals would rapidly lead to freezing of the large drops through collision and ice multiplication processes. For MVD $< 40 \mu\text{m}$, the probability of exceeding $12 \text{ g cm}^{-2} \text{ h}^{-1}$ was 0.3% for liquid-phase conditions, while such conditions were not observed for mixed-phase conditions. Liquid-phase conditions accounted for 10 of 12 observed cases with LWC $> 0.6 \text{ g m}^{-3}$. The co-existence of high LWC and ice crystals would lead to rapid growth of the ice crystals through

riming and vapour deposition, which would reduce the total LWC and hence the potential accumulation. The total water content (TWC) of liquid and mixed-phase icing environments were quite similar, with 50% and 95% values of approximately 0.13 and 0.36 g m^{-3} respectively. These observations are based on analysis of the cloud conditions observed in the research flights reported here, and should not be generally extended to represent all mixed-phase cloud conditions.

INTRODUCTION

The 1997 Federal Aviation Administration (FAA) Inflight Aircraft Icing Plan contains explicit recommendations to consider a comprehensive redefinition of the current aircraft icing certification envelopes when sufficient information is available worldwide on supercooled large drops (SLD), mixed-phase icing conditions and other icing conditions. This has in part generated substantial research efforts towards characterizing aircraft icing environments associated with SLD. Recent research projects focusing on this problem have included the Winter Icing Storms Project (Rasmussen et al. 1992¹), the Canadian Freezing Drizzle Experiments (Isaac et al. 2001²), the NASA winter icing projects (Miller et al. 1998³) and the Alliance Icing Research Study (Isaac et al. 2001⁴). These projects have generated a large quantity of high quality in-situ measurements, and include substantial numbers of observations in liquid and mixed-phase icing conditions. While analysis of the liquid-phase conditions has, in part, been reported in Cober et al. (2001⁵), Politovich and Bernstein (2002⁶), and Miller et al. (1998³), there has been little progress in characterizing mixed-phase clouds. This is because of the difficulty in separating ice and liquid hydrometeor responses on most of the instruments used for cloud measurements. As a consequence, despite extensive characterisations of aircraft icing and SLD environments (Sand et al. 1984⁷; Cooper et al. 1984⁸; Politovich 1989⁹; Pobanz et al. 1994¹⁰; Cober et al. 1996¹¹, 2001⁵; Ashenden and Marwitz 1998¹²; Miller et al. 1998³), there have been no similar attempts to provide an in-depth characterization of mixed-phase icing conditions, even though they are often discussed (Strapp et al. 1999¹³; Cober et al. 1995¹⁴, 2001⁵; Bain and Gayet 1982¹⁵; Korolev et al. 2002¹⁶). Korolev and Isaac (2002¹⁷)

Copyright © 2002 by Environment Canada. Published by the American Institute of Aeronautics and Astronautics, Inc. with permission.

examined theoretically the formation and life cycle of mixed-phase clouds and found that under some conditions, mixed-phase conditions could be maintained for time scales of hours. This further highlights the importance of characterizing mixed-phase icing conditions. Riley (1998¹⁸) provided a review of measurements of mixed-phase icing conditions, and found that mixed-phase conditions in clouds with temperatures $\leq 0^{\circ}\text{C}$ were observed with a frequency of between 20 and 90%, depending on the temperature, environment, region and instrumentation. He concluded that assessing mixed-phase icing conditions was an important research objective. To address this, Cober et al. (2001¹⁹) summarized the relative responses to ice and water hydrometeors for several instruments used by the Meteorological Service of Canada. This evaluation methodology was used to differentiate liquid, mixed and glaciated cloud conditions, and to assess the microphysics associated with each. This paper provides a characterization of icing environments that were observed in mixed-phase cloud conditions, as based on in-situ measurements made during four research field projects. The characterizations are then compared to similar analysis for liquid-phase icing conditions.

Characterising mixed-phase cloud conditions has other important applications including climate research, numerical forecast modelling, radiative transfer, cloud microphysics processes, precipitation formation and remote sensing. Each of these topics requires accurate in-situ measurements of both the liquid and ice hydrometeors in mixed-phase conditions.

FIELD PROJECTS

The data were obtained during several field projects including the First and Third Canadian Freezing Drizzle Experiments (CFDE I and CFDE III respectively), the Alliance Icing Research Study (AIRS), and the First ISCCP Regional Experiment Arctic Cloud Experiment (FIRE.ACE). CFDE I was conducted in March 1995 and consisted of 12 flights over Newfoundland and the North Atlantic Ocean (Isaac et al. 2001²). CFDE III was conducted between December 1997 and February 1998, and consisted of 26 flights over Southern Ontario and Quebec, Lake Ontario and Lake Erie (Isaac et al. 2001²). FIRE.ACE was conducted during April 1998, and included 18 flights over the Beauford Sea and Inuvik regions of the Canadian Arctic (Gultepe and Isaac 2002²⁰). Finally, AIRS was conducted between December 1999 and February 2000 and included 25 flights in the same geographic region as CFDE III (Isaac et al. 2001⁴). A primary research objective of CFDE I, CFDE III, and AIRS was to collect in-situ measurements to characterize

aircraft icing environments. FIRE.ACE was designed to study Arctic boundary layer cloud, and a significant portion of the in-flight time during each project was made in cloud at temperatures $\leq 0^{\circ}\text{C}$. Overall, this collective data set includes approximately 32,000 km of in-cloud measurements at temperatures $\leq 0^{\circ}\text{C}$, the majority of which were associated with winter storms. Numerous observations of liquid and mixed-phase cloud conditions make the data set well suited for assessing and comparing the icing environments associated with each phase.

INSTRUMENTATION

Data presented here were obtained with the National Research Council (NRC) Convair-580 aircraft. This aircraft and its instrumentation suite have been described in Cober et al. (1995¹⁴), Isaac et al. (2001²), and Cober et al. (2001⁵). The instrumentation remained relatively unchanged through all the projects. The Convair-580 contained sufficient instrumentation to measure the essential cloud microphysical parameters including temperature, liquid water content, total water content, droplet/SLD/ice crystal concentrations and sizes.

Cober et al. (2001¹⁹) provides an in-depth assessment of the capabilities of the instrumentation on the Convair-580 in liquid, mixed and glaciated-phase cloud conditions. They assessed the relative responses to ice and liquid hydrometeors for several instruments, including a Rosemount icing detector (Cober et al. 2001²¹), PMS 2D-C mono and 2D-C grey probes, PMS FSSP on three separate measurement ranges, Nevzorov liquid water content (LWC) and total water content (TWC), and PMS King LWC probes.

DATA ANALYSIS

The data from each flight were initially averaged in sequential 30-second intervals, corresponding to a horizontal length scale of 2.9 ± 0.3 km where the error represents the standard deviation on the mean. The 30-s averaging scale was chosen because it represented a short averaging scale that generally allowed sufficient 2D measurements for statistical significance. For each interval, droplet data from the FSSP and 2D probes were combined to interpolate a normalized drop spectrum from 1 micron to the maximum observed drop diameter. For each droplet spectrum, the LWC and median volume diameter (MVD) were computed for comparison to the icing envelop formulations of FAR 25-C²² and Newton (1978²³). For those spectra measured at a temperature $\leq 0^{\circ}\text{C}$, the drops larger than 50 μm in diameter will be collectively referred to as SLD. For each 30-s interval, ice crystal measurements from the 2D-C and 2D-P probes

were used to determine an ice crystal spectrum from 125 μm to the maximum ice crystal diameter observed. Ice crystals smaller than 125 μm in diameter could not be accurately measured with any of the 2D instruments because of depth of field and sizing uncertainties that exist for these sizes (Korolev et al. 1998²⁴, Strapp et al. 2001²⁵). The FSSPs were not used to estimate the ice crystal sizes.

Cober et al. (2001¹⁹) identified the phase for each 30-second interval as being liquid, mixed or glaciated. Liquid-phase cases were identified using several criteria including: the fraction of processed 2D images ($\geq 125 \mu\text{m}$) that were circular > 0.85 ; visual examination of the 2D imagery indicating no or very few ice particles; concentration of irregular (i.e. ice crystals) images $< 0.1 \text{ L}^{-1}$ as measured with the 2D probes; agreement between the LWC instruments within $\pm 15\%$; and agreement between the LWC and TWC measurements within $\pm 15\%$ except in cases with significant mass in drops $> 100 \mu\text{m}$. For liquid-phase conditions, the entire FSSP spectra, 2D-C spectra $\geq 125 \mu\text{m}$ and 2D-P spectra $\geq 1000 \mu\text{m}$ were used to produce the integrated drop spectra.

Mixed-phase conditions were identified when the instruments collectively demonstrated all of the following characteristics: ratio of LWC to TWC between 0.2 and 1.0; fraction of circular 2D images $\geq 125 \mu\text{m}$ between 0.4 and 0.9; FSSP concentrations $> 15 \text{ cm}^{-3}$; visual assessment that the 2D images contained ice crystals; and a RID response $> 2 \text{ mV s}^{-1}$ (for temperatures $< -4^\circ\text{C}$). For mixed-phase conditions with ice crystal concentrations of $> 1 \text{ L}^{-1}$ (for sizes $\geq 125 \mu\text{m}$) the FSSP measurements were assessed to include ice particles, and hence were considered unreliable for sizing droplets at sizes $> 35 \mu\text{m}$ (Cober et al. 2001¹⁹). This observation was similar for two FSSP instruments, regardless of the measurement range. Therefore, FSSP measurements were not used to infer droplet sizes $> 35 \mu\text{m}$, whenever the ice crystal concentration $> 1 \text{ L}^{-1}$. Glaciated conditions were assessed when there were no supercooled water drops detected with any of the instruments.

RESULTS

There were 81 research flights conducted during the four field projects. These provided approximately 37,000 in-flight data points averaged at 30-s resolution, of which 30% were assessed as being in-cloud at a temperature $\leq 0^\circ\text{C}$. For the 10849 in-cloud observations with a temperature $\leq 0^\circ\text{C}$, the relative fraction of liquid, mixed and glaciated conditions were 0.35, 0.43 and 0.22 respectively. While this suggests that liquid and mixed-phase conditions were observed

with a roughly equal frequency, the temperatures at which the data were collected bias these values. Figure 1 shows the in-cloud frequency of occurrence of liquid, mixed and glaciated-phase cases as a function of temperature. The fraction of glaciated-phase conditions is a minimum near 0°C , and increases with decreasing temperature, while the fraction of liquid-phase conditions is a maximum near 0°C and decreases with decreasing temperature. These trends are consistent with an increasing probability for heterogeneous ice nucleation with decreasing temperature. There is a peak in the frequency of glaciated conditions at -15°C , which is possibly associated with the maximum in the saturation vapour pressure difference between ice and water. The fraction of mixed-phase cases is relatively constant from 0 to -30°C . At the colder temperatures, this may reflect a bias in the research flights, which were designed to measure icing conditions, and which were directed towards regions where supercooled liquid water was known or forecast to exist. The data in Figure 1 suggest that, at all temperatures colder than -5°C , mixed-phase cloud conditions will be more frequent than liquid-phase conditions. This has implications for remote sensing of icing conditions with instruments such as radars, where the signal will in general be dominated by the largest hydrometeors, and for microphysics parameterization schemes used in icing forecast models, where the ice processes being simulated are sensitive to the cloud temperature. If it is assumed that there is an equal probability of encountering a cloud at any temperature between 0 and -30°C , and that the curves in Figure 1 represent the relative frequencies of occurrence of liquid, mixed and glaciated-phase conditions as a function of temperature, the average frequencies of occurrence of liquid, mixed and glaciated-phase conditions would be 0.20, 0.48 and 0.32 respectively.

The total water content of each 30-s interval was determined with a Nevzorov TWC probe (Korolev et al. 1998²⁶). Cumulative TWC probability curves for liquid, mixed and glaciated-phase conditions are shown in Figure 2. For liquid-phase conditions, the TWC represents the LWC because the ice water content (IWC) is essentially zero (ice water fraction < 0.05), while for glaciated-phase conditions the TWC represents the IWC because the LWC is essentially zero ($< 0.01 \text{ g m}^{-3}$) (Cober et al. 2001¹⁹). The median (50%) values of TWC were 0.13, 0.12 and 0.10 g m^{-3} for the liquid, mixed and glaciated-phase conditions respectively, while the 95% probability values were 0.38, 0.34 and 0.26 g m^{-3} . Clearly, higher TWC values were observed at a lower frequency in glaciated conditions than in liquid or mixed conditions. This is primarily related to temperature. Figure 3 shows the

TWC as a function of temperature for several percentile values of TWC. There is a systematic decrease in the mean TWC with temperature, which is consistent with previous observations (Gultepe and Isaac 1997²⁷; Korolev et al 2001²⁸). The 95% probability curve is essentially flat from 0 to -15°C . The mean temperatures for liquid, mixed and glaciated-phase conditions for the data presented here were -5.2 , -8.1 and -10.9°C respectively. The lower mean temperature for glaciated conditions is consistent with the lower mean TWC values observed for glaciated conditions. It may also reflect biases in the research flight methodology, since deep glaciated cloud regions were avoided since they were unlikely to contain icing conditions.

An important observation in Fig. 2 is the similarity between the liquid and mixed-phase conditions. Since the probability curves for liquid and mixed-phase are essentially the same, this implies that the net TWC available for icing on an airframe will not be significantly different in mixed-phase conditions relative to liquid-phase conditions. The nature of the ice growth may be different, depending on whether or not ice crystals are incorporated into the growing ice surface. Similarly, the amount of mass available for ice formation may be slightly different depending on the relative collision efficiencies for drops and ice crystals. Answers to these questions are beyond the scope of this paper. Hallett and Isaac (2002²⁹) discuss some of these issues in more detail. However, neglecting any differences in the collision efficiencies for ice crystals and water drops, Figure 2 implies that thermal anti-icing systems that are certified for FAR 25-C liquid-phase conditions should be adequate for TWC conditions found in mixed-phase clouds, for the stratiform winter clouds examined in this study.

The net LWC available for icing on an airframe will be different for liquid and mixed-phase clouds. This is demonstrated in Figure 4, which shows cumulative probability curves for LWC for liquid and mixed-phase conditions as a function of liquid water fraction. Liquid water fraction is defined as the ratio of the LWC to TWC. As the liquid water fraction decreases, the 95% LWC decreases. The curves for liquid-phase clouds and for mixed-phase clouds with liquid water fractions close to 1 are essentially identical. Mixed-phase clouds with liquid fractions > 0.9 accounted for 55% of the observed mixed-phase conditions. These clouds primarily contained two distinct particle types, cloud drops with substantial LWC, and ice crystals with a collective small IWC. These ice crystals tended to be relatively large ($> 200\ \mu\text{m}$) which would be expected since crystals in a water saturated environment

will generally grow rapidly by vapour deposition. It is likely that the ice crystals would grow to a point where they would fall out relative to the cloud drops. In the absence of an ice multiplication mechanism, it is suggested that these clouds could maintain a high liquid water fraction for a substantial time period. This would, in part, explain the observed high frequency of mixed-phase clouds with high liquid water fractions.

The average droplet and SLD spectra from liquid-phase cloud conditions, and the average ice crystal spectra from glaciated conditions, are shown in Figure 5. These represent averages over the collective data set. The slopes of the drop (liquid) and ice crystal (glaciated) spectra are substantially different. For comparison, the average drop spectra for mixed-phase clouds with ice crystal concentrations $< 1\ \text{L}^{-1}$ (mixed-liquid), and the average ice crystal spectra for mixed-phase clouds with ice crystal concentrations $> 1\ \text{L}^{-1}$ (mixed-ice), are also shown in Figure 5. For each of the mixed-liquid and mixed-ice spectra, the mixed-phase conditions were segregated by ice crystal concentration to avoid large errors in the instrument interpretations. The drop (mixed-liquid) and ice crystal (mixed-ice) spectra observed in the mixed-phase clouds are remarkably similar to those from the liquid and glaciated-phase clouds respectively, suggesting that the mean spectra from the liquid and glaciated conditions can be considered as representative of mixed-phase conditions. If collision efficiency curves were applied to each spectrum, these might be used to compute differences in mass loading for thermal de-icing systems for liquid, mixed and glaciated-phase conditions.

Figures 6 and 7 show LWC versus MVD for each 30-s droplet spectra for liquid and mixed-phase conditions respectively. These are compared to the Newton (1978²³) potential icing accumulation envelopes of 1, 6 and $12\ \text{g cm}^{-2}\ \text{h}^{-1}$. For the mixed-phase conditions, the data are segregated by ice crystal concentration for concentrations $< 1\ \text{L}^{-1}$ and concentrations between 1 and $3\ \text{L}^{-1}$. The MVD for the spectra with ice concentrations between 1 and $3\ \text{L}^{-1}$ have a greater uncertainty because the FSSP drop spectra measurements are biased whenever the ice crystal concentration exceeds $1\ \text{L}^{-1}$ (Cober et al. 2001¹⁹). These data are not used for the following analysis, and they are shown in Figure 7 only for comparison. In total 10.3% of the liquid-phase conditions had a potential accumulation of $> 6\ \text{g cm}^{-2}\ \text{h}^{-1}$, compared to only 4.5% of the mixed-phase conditions. The liquid and mixed-phase cases with $\text{MVD} < 40\ \mu\text{m}$ appear similar. However, the frequency of exceeding $12\ \text{g cm}^{-2}\ \text{h}^{-1}$

¹ was 0.34% for the liquid-phase cases, while no similar mixed-phase cases were observed. For $MVD > 40 \mu\text{m}$ there is a more dramatic difference in the liquid and mixed-phase cases. Every case with a $MVD > 70 \mu\text{m}$ and potential accumulation $> 6 \text{ g cm}^{-2} \text{ h}^{-1}$ was liquid-phase. Finally, for icing conditions with $MVD > 400 \mu\text{m}$, the relative fractions of liquid and mixed-phase conditions were 0.98 and 0.02 respectively. These conditions were primarily observed below a melting layer in classical freezing rain conditions, where the ambient temperatures were warm enough ($> -5^\circ\text{C}$) to significantly restrict the formation of ice crystals by heterogeneous nucleation. This minimized the frequency of occurrence of mixed-phase conditions for these cases.

Qualitatively, at the extreme values of LWC and MVD, there appears to be significant differences between the liquid and mixed-phase conditions. To quantify these observations, the data were segregated by increasing MVD, into bins of 100 data points. For each bin, the 98, 99 and 100% LWC values were determined. This is a similar methodology to that done for the FAR 25-C curves, except that this data was not further segregated by temperature, and represents a shorter horizontal extent than the FAR 25-C data. The results for liquid and mixed-phase conditions are shown in Figures 8 and 9 respectively, and are compared to the Newton (1978²³) potential accumulation envelopes and the FAR 25-C curves for 0, -10 and -20°C . The error bars represent the MVD range for each bin, and the 98 to 100% range of LWC values for each bin. For $MVD > 20 \mu\text{m}$, the curves for the liquid-phase conditions follow the potential accumulation curve of approximately $10 \text{ g cm}^{-2} \text{ h}^{-1}$. It is not surprising that the shape of the liquid-phase curve is relatively flat at $MVD > 100 \mu\text{m}$ because the collision efficiency is essentially 1 at these sizes and LWC should be relatively independent of MVD. For $MVD < 50 \mu\text{m}$ the liquid and mixed-phase data are quite similar, although the liquid-phase data have higher LWC values around $30 \mu\text{m}$. For high LWC values, ice crystals would grow rapidly by riming which would reduce the available LWC. For $MVD > 50 \mu\text{m}$, there are only 50 mixed-phase data points, and the LWC values are significantly smaller than for the liquid-phase conditions with $MVD > 50 \mu\text{m}$. For mixed-phase conditions at high MVD values, the ice crystals would have higher collision efficiencies with drizzle-sized drops, which in turn may enhance any ice multiplication processes. Hence, the presence of ice crystals in a high MVD environment could result in the freezing of drizzle-sized drops, which would lower the LWC and MVD. Increased collision efficiency of large drops with ice crystals, and the relationship between large drops and ice multiplication (Hallett and Mossop 1974³⁰) are consistent with this hypothesis.

To further highlight the differences between liquid and mixed-phase conditions with respect to MVD, the collective liquid and mixed-phase data set for conditions with temperatures $\leq 0^\circ\text{C}$ and ice crystal concentrations $< 1 \text{ L}^{-1}$ were segregated into MVD bins of 100 data points. Note that this subset ignores 54% of the mixed-phase conditions where the ice crystal concentration $> 1 \text{ L}^{-1}$, because the drop spectra cannot be accurately measured between 35 and $275 \mu\text{m}$ in these cases (Cober et al. 2001¹⁹). The relative fractions of liquid and mixed-phase conditions were determined for each MVD bin for increasing MVD. The MVD values were based only on the measured drop spectra. The results are shown in Figure 10. This subset of data had average liquid and mixed-phase fractions of 0.62 and 0.38 respectively. For $MVD < 20 \mu\text{m}$, the relative frequency of liquid and mixed conditions were approximately equal. However, the relative frequency of liquid-phase conditions increased with increasing MVD for $MVD > 20 \mu\text{m}$. For $MVD > 40 \mu\text{m}$, liquid-phase conditions accounted for in excess of 80% of the observed cloud conditions where LWC was present. A similar analysis was done segregating the data using LWC and the results are shown in Figure 11. Here, the LWC values are based only on the drop spectra. There is no change in the relative fractions of liquid or mixed-phase conditions with increasing LWC. This is consistent with the results of Figure 2. Using a bin size of 100 data points masked the fact that 10 of the 12 cases with $LWC > 0.6 \text{ g m}^{-3}$ were liquid-phase.

CONCLUSIONS

Measurements of liquid and mixed-phase icing environments were made during 81 research flights conducted during four field projects. In total, there were 10,849 30-second in-cloud measurements obtained with temperatures $\leq 0^\circ\text{C}$. The majority of data were collected in stratiform winter clouds. The analysis has led to the following conclusions:

1. The relative fractions of liquid, mixed and glaciated-phase conditions were 0.35, 0.43 and 0.22 respectively. When the results were normalized by temperature, assuming that temperatures between 0 and -30°C were equally probable, the relative frequencies of liquid, mixed and glaciated conditions were 0.20, 0.48 and 0.32 respectively. Mixed-phase icing conditions were frequently observed during the research flights, and were more frequent than liquid-phase conditions at all temperatures colder than -5°C . Approximately 55% of the mixed-phase observations had a liquid fraction > 0.9 . These conditions generally

contained two distinct hydrometeor distributions, a cloud droplet distribution that incorporated the bulk of the TWC, and an ice crystal distribution that incorporated a small IWC.

2. The total water contents of liquid and mixed-phase conditions were observed to be very similar, with 50% and 95% probability values of approximately 0.13 and 0.36 g m⁻³ respectively. Neglecting the differences in collision efficiencies between drops and ice crystals, this implies that for cloud conditions similar to those reported here, thermal de-icing systems that have been tested and certified in liquid-phase conditions should perform acceptably in mixed-phase conditions. The average drop and ice crystal spectra observed in mixed-phase clouds were very similar to those observed in liquid and glaciated clouds respectively, suggesting that the latter measurements could be considered representative of those in mixed-phase conditions. Characteristic drop, SLD and ice spectra are presented, from which mass impingement could be computed, given the corresponding collision efficiencies.

3. There are significant differences in icing environments associated with mixed and liquid-phase conditions. While there was no substantial difference in the relative frequencies of liquid and mixed-phase conditions with increasing LWC, for LWC > 0.6 g m⁻³, liquid conditions accounted for 10 of the 12 data points observed. Presumably, when ice crystals exist in a high LWC environment, they will grow rapidly through riming and vapour deposition, which will reduce the available LWC. The relative fraction of liquid-phase conditions increased with increasing MVD for conditions with MVD > 20 μm, and for MVD > 40 μm 80% of the observed icing cases were liquid-phase. For drop spectra with MVD > 70 μm, there were no mixed-phase cases with potential accumulations > 6 g cm⁻² h⁻¹, while 14% of the liquid-phase cases with > 6 g cm⁻² h⁻¹ had MVD > 70 μm. It is suggested that ice crystals co-existing with SLD will lead to glaciation of the SLD through collision and ice multiplication. For icing conditions with MVD > 400 μm, 98% were associated with liquid-phase conditions. These were primarily associated with freezing rain below a melting layer, for which the associated warm ambient temperatures restricted the development of ice crystals through heterogeneous nucleation. Hence, while mixed-phase conditions were more frequently observed than liquid-phase conditions at all temperatures < -5°C, the high LWC, high potential accumulation from liquid water, and high MVD conditions tended to be significantly more frequent in liquid-phase conditions.

4. There are regional differences in the relative frequencies of liquid, mixed and glaciated-phase clouds. For example, maritime clouds observed in CFDE I, with temperatures between 0 and -20°C, had normalized glaciated and mixed-phase frequencies of 0.53 and 0.21 respectively, compared with 0.24 and 0.50 respectively for the continental cases observed during CFDE III and AIRS. In addition, the icing characteristics in different cloud types (e.g. tops of cumulonimbus clouds, see Strapp et al. 1999¹³) would be expected to be quite different than those observed in the winter stratiform clouds reported here.

5. The fact that mixed-phase conditions occur more frequently than all liquid conditions is important for icing simulation studies. There are relatively few wind tunnel and CFD simulations with mixed-phase conditions, and in-flight measurements of simultaneous droplet and ice crystal impingements on aircraft (Hallett and Isaac 2002²⁹) are also rare. Such studies are difficult because a multi-phase environment would need to be considered, and ice crystal collision efficiencies and sticking coefficients are not well known. Regardless, it is recommended that further in-flight, wind tunnel and CFD studies be performed to assess the importance of ice crystals for icing on aircraft structures within mixed-phase clouds.

ACKNOWLEDGEMENTS

The Canadian National Search and Rescue Secretariat, Transport Canada, the National Research Council (NRC), the Meteorological Service of Canada (MSC), and Boeing Commercial Airplane Group supported this research. The authors would like to thank Walter Strapp, Alexei Korolev and Ismail Gultepe for discussions during the analysis.

REFERENCES

1. Rasmussen, R., M. Politovich, J. Marwitz, W. Sand, J. McGinley, J. Smart, R. Pielke, S. Rutledge, D. Wesley, G. Stossmeister, B. Bernstein, K. Elmore, N. Powell, E. Westwater, B.B. Stankov, and D. Burrows, 1992: Winter icing and storms project (WISP). *Bull. Amer. Meteorol. Soc.*, **73**, 951-974.
2. Isaac, G.A., S.G. Cober, J.W. Strapp, A.V. Korolev, A. Tremblay, and D.L. Marcotte, 2001: Recent Canadian research on aircraft in-flight icing. *Canadian Aeronautics and Space Journal*, **47**, 213-221.
3. Miller, D., T. Ratvasky, B. Bernstein, F.

- McDonough, and J.W. Strapp, 1998: NASA/FAA/NCAR supercooled large droplet icing flight research: Summary of winter 96-97 flight operations. *AIAA 36th Aerospace Sci. Meeting and Exhibit*, Reno Nevada, 12-15 January 1998, Paper 98-0577.
4. Isaac, G.A., S.G. Cober, J.W. Strapp, D. Hudak, T.P. Ratvasky, D.L. Marcotte, and F. Fabry, 2001: Preliminary results from the Alliance Icing Research Study (AIRS). *AIAA 39th Aerospace Sci. Meeting and Exhibit*, Reno Nevada, 8-11 January 2001, AIAA 2001-0393.
 5. Cober, S.G., G.A. Isaac, and J.W. Strapp, 2001: Characterizations of aircraft icing environments that include supercooled large drops. *J. Appl. Meteor.*, **40**, 1984-2002.
 6. Politovich, M.K., and T.A. Bernstein, 2002: Aircraft icing conditions in northeast Colorado. Accepted to *J. Appl. Meteor.*
 7. Sand, W.R., W.A. Cooper, M.K. Politovich, and D.L. Veal, 1984: Icing conditions encountered by a research aircraft. *J. Climate Appl. Meteor.*, **23**, 1427-1440.
 8. Cooper, W.A., W.R. Sand, M.K. Politovich, and D.L. Veal, 1984: Effects of icing on performance of a research aircraft. *J. Aircraft*, **21**, 708-715.
 9. Politovich, M.K., 1989: Aircraft icing caused by large supercooled droplets. *J. Appl. Meteor.*, **28**, 856-868.
 10. Pobanz, B.M., J.D. Marwitz, and M.K. Politovich, 1994: Conditions associated with large-drop regions. *J. Appl. Meteor.*, **33**, 1366-1372.
 11. Cober, S.G., J.W. Strapp, and G.A. Isaac, 1996: An example of supercooled drizzle drops formed through a collision-coalescence process. *J. Appl. Meteor.*, **35**, 2250-2260.
 12. Ashenden, R., and J.D. Marwitz, 1998: Characterizing the supercooled large droplet environment with corresponding turboprop aircraft response. *J. Aircraft*, **35**, 912-920.
 13. Strapp, J.W., P. Chow, M. Maltby, A.D. Bezer, A.V. Korolev, I. Stromberg, and J. Hallett, 1999: Cloud microphysical measurements in thunderstorm outflow regions during Allied/BAE 1997 flight trials. *AIAA 37th Aerospace Sci. Meeting and Exhibit*, Reno Nevada, 11-14 January 1999, Paper 99-0498.
 14. Cober, S.G., G.A. Isaac, and J.W. Strapp, 1995: Aircraft icing measurements in east coast winter storms. *J. Appl. Meteor.*, **34**, 88-100.
 15. Bain, M., and J.F. Gayet, 1982: Aircraft measurements of icing in supercooled and water droplet/ice crystal clouds. *J. Appl. Meteor.*, **21**, 631-641.
 16. Korolev, A.V., G.A. Isaac, S.G. Cober, J.W. Strapp and J. Hallett, 2002: Observations of the microstructure of mixed-phase clouds. Submitted to *Q. J. Roy. Meteor. Soc.*
 17. Korolev, A.V., and G.A. Isaac, 2002: Phase transformation in mixed-phase clouds. Submitted to *Q. J. Roy. Meteor. Soc.*
 18. Riley, R.K., 1998: Mixed-phase icing conditions: A review. U.S. Dept. of Transportation Report DOT/FAA/AR-98/76, 45 pp.
 19. Cober, S.G., G.A. Isaac, A.V. Korolev, and J.W. Strapp, 2001: Assessing cloud-phase conditions. *J. Appl. Meteor.*, **40**, 1967-1983.
 20. Gultepe, I., and G.A. Isaac, 2002: The effects of air-mass origin on Arctic cloud microphysical parameters during FIRE.ACE. Accepted to *J. Geophys. Res.*
 21. Cober, S.G., G.A. Isaac, and A.V. Korolev, 2001: Assessing the Rosemount icing detector with in-situ measurements. *J. Atmos. Oceanic Technol.*, **18**, 515-528.
 22. Federal Aviation Administration, 1999: U.S. Code of Federal Regulations, Title 14 (Aeronautics and Space), Part 25 (Airworthiness Standard: Transport Category Airplanes), Appendix C, National Archives and Records Administration, U.S. Government Printing Office, Washington D.C.
 23. Newton, D.W., 1978: An integrated approach to the problem of aircraft icing. *J. Aircraft*, **15**, 374-380.
 24. Korolev, A.V., J.W. Strapp, and G.A. Isaac, 1998: Evaluation of the accuracy of PMS optical array probes. *J. Atmos. Oceanic Technol.*, **15**, 708-720.
 25. Strapp, J.W., F. Albers, A. Reuter, A.V. Korolev, W. Maixner, E. Rashke, and Z. Vukovic, 2001: Laboratory measurements of the response of a PMS OAP-2DC probe. *J. Atmos. Oceanic Technol.*, **18**, 1150-1170.
 26. Korolev, A.V., J.W. Strapp, G.A. Isaac, and A.N. Nevzorov, 1998: The Nevzorov airborne hot-wire

LWC-TWC probe: Principles of operation and performance characteristics. *J. Atmos. Oceanic Tech.*, **15**, 1495-1510.

27. Gultepe, I., and G.A. Isaac, 1997: Relationship between liquid water content and temperature based on aircraft observations and its applicability to GCMs. *J. Climate*, **10**, 446-452.

28. Korolev, A.V., G.A. Isaac, I.P. Mazin, and H. Barker, 2001: Microphysical properties of continental stratiform clouds. *Q. J. Roy. Meteor. Soc.*, **127**, 2117-2151.

29. Hallett, J., and G.A. Isaac, 2002: Aircraft icing in glaciated and mixed phase clouds. *AIAA 40th Aerospace Sci. Meeting and Exhibit*, Reno Nevada, 14-17 January 2002, AIAA 2002-0677.

30. Hallett, J., and S.C. Mossop, 1974: Production of secondary ice particles during the riming process. *Nature*, **249**, 26-28.

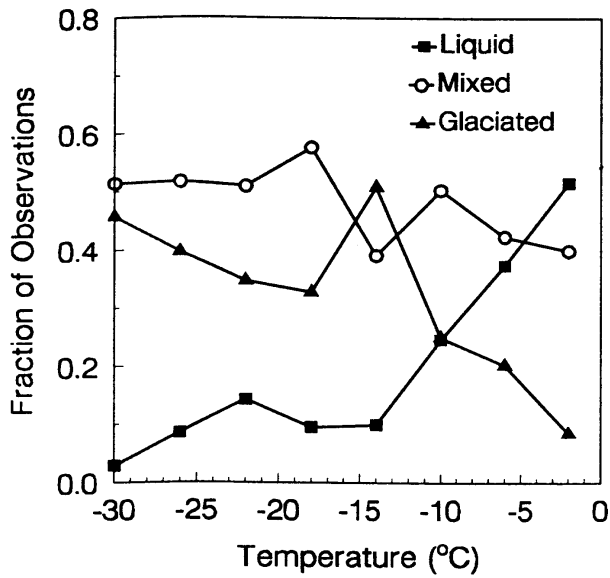


Figure 1. Relative frequencies of occurrence of liquid, mixed and glaciated-phase conditions as a function of temperature. The data were segregated into temperature intervals of 4°C. The analysis is based on 10,500 in-cloud points with TWC > 0.01 g m⁻³ and temperature ≤ 0°C.

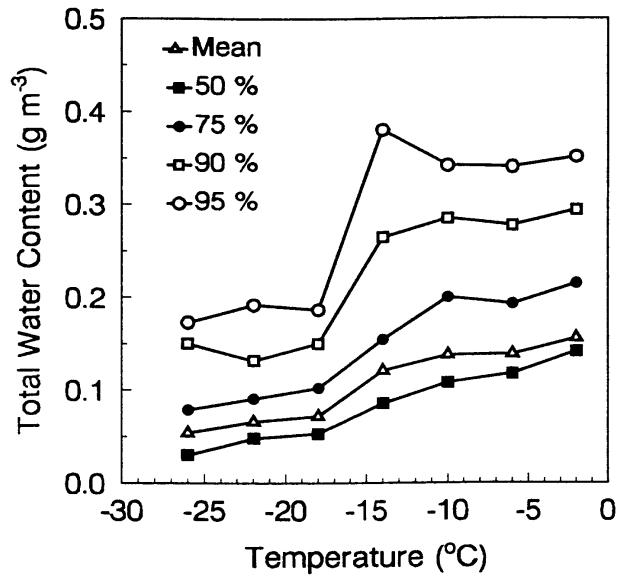


Figure 3. Curves of constant TWC percentile, as a function of temperature. The data includes all liquid, mixed and glaciated-phase conditions with TWC > 0.005 g m⁻³ and temperature ≤ 0°C. The curves represent the mean, 50, 75, 90 and 95 percentiles of TWC.

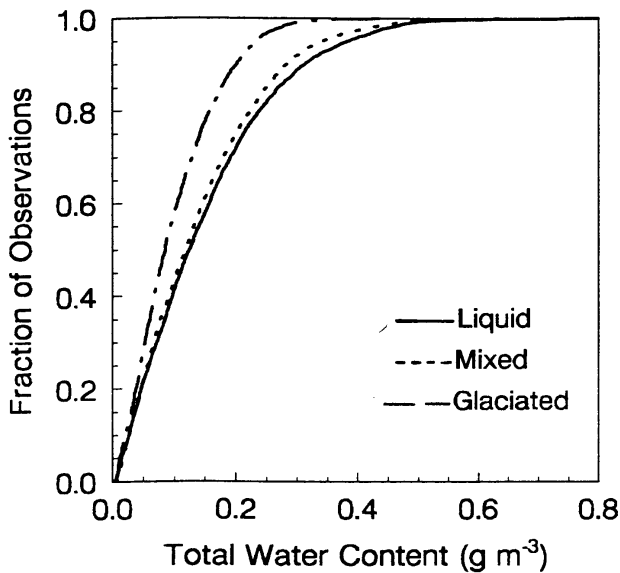


Figure 2. Cumulative probability curves of TWC as a function of cloud-phase for cloud conditions with TWC > 0.005 g m⁻³ and temperature ≤ 0°C. The data are based on 3765, 4695, and 2331 liquid, mixed and glaciated cases respectively.

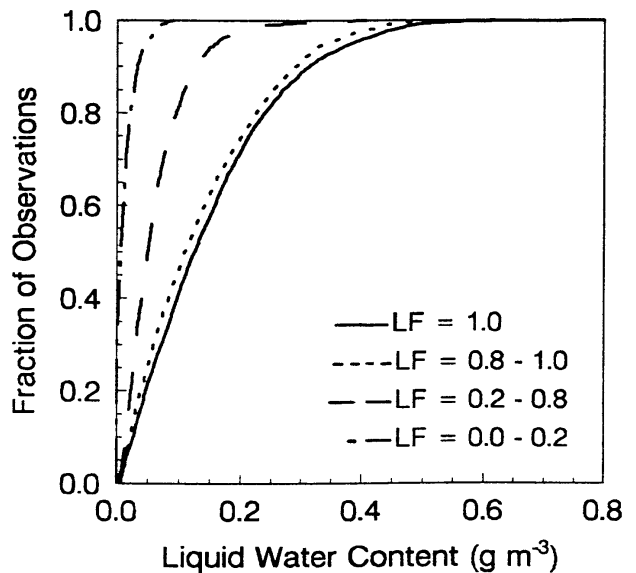


Figure 4. Cumulative probability curves of LWC as a function of liquid fraction (LF) for liquid (LF = 1.0) and mixed-phase conditions.

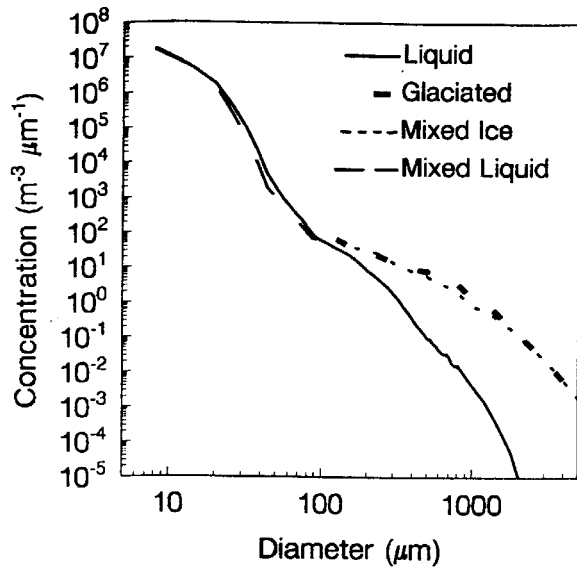


Figure 5. Average drop, SLD, and ice crystal spectra for liquid, mixed and glaciated-phase conditions. The drop and SLD spectra are based on 2037 liquid-phase conditions. The average ice crystal spectrum is based on 1368 glaciated-phase conditions. The average mixed-phase drop spectrum (Mixed Liquid) is based on 1664 cases with ice concentrations $< 1 \text{ L}^{-1}$, while the average mixed-phase ice crystal spectrum (Mixed Ice) is based on 1760 cases,

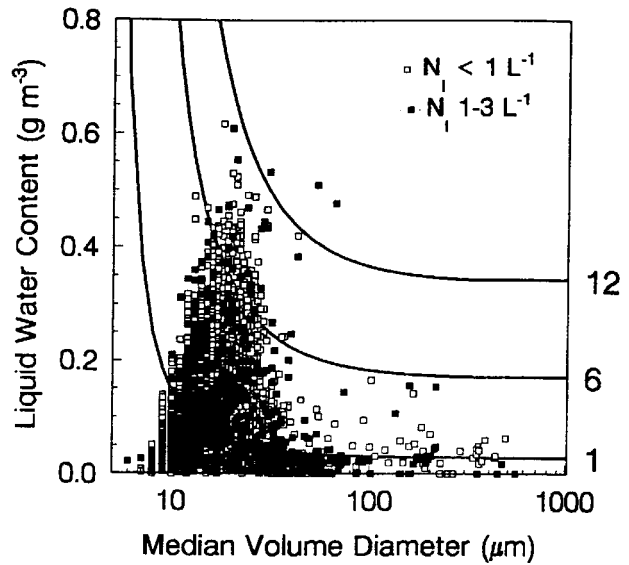


Figure 7. Plot of the droplet spectrum MVD versus LWC for each 30-s observation made in mixed-phase clouds. The data are segregated for ice crystal concentrations (N_i) $< 1 \text{ L}^{-1}$ and $1-3 \text{ L}^{-1}$.

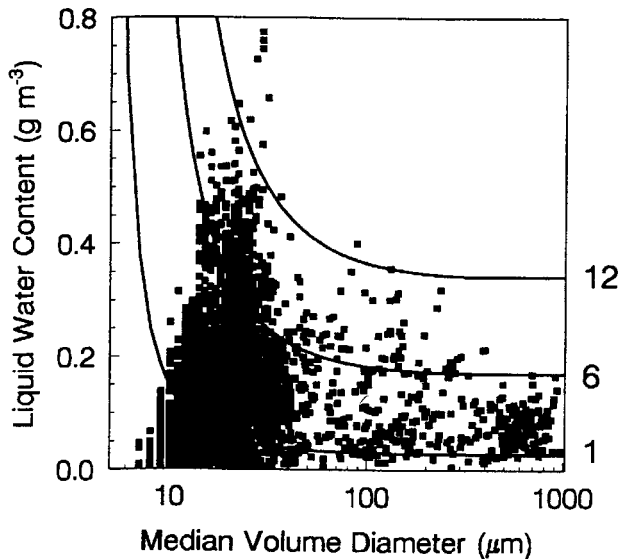


Figure 6. Plot of the droplet spectrum MVD versus LWC for each 30-s observation made in liquid-phase clouds with ice crystal concentrations $< 1 \text{ L}^{-1}$. The solid curves represent potential accumulation curves for 1, 6 and $12 \text{ g cm}^{-2} \text{ h}^{-1}$, as defined by Newton (1978²³).

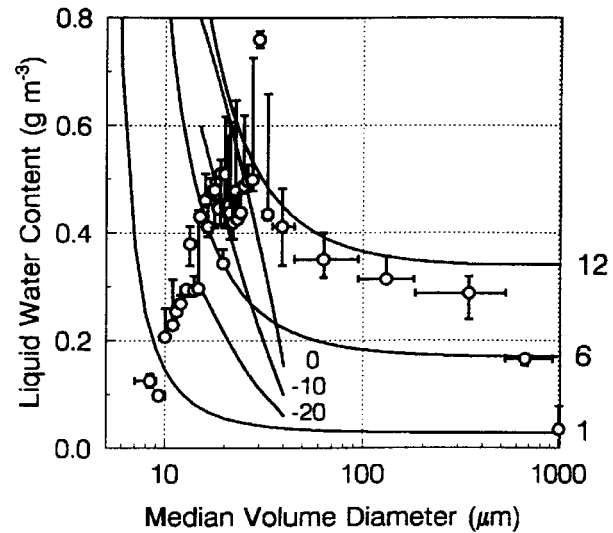


Figure 8. Plot of MVD versus LWC for the liquid-phase cases. The data were segregated by MVD into bins of 100 data points. Each MVD data point shows the average MVD for the bin, along with a range from the maximum to the minimum MVD for the bin. Each LWC data point shows the 99% LWC value, along with a range from the 98% to the 100% LWC values for the bin. The analysis is based on 3502 liquid-phase data points.

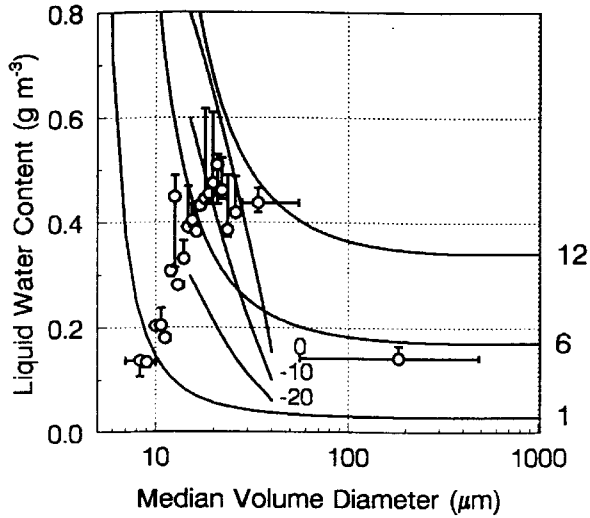


Figure 9. Same as for Figure 8, except for mixed-phase cases with ice crystal concentrations $< 1 \text{ L}^{-1}$. The analysis is based on 2150 mixed-phase data points. Potential accumulation curves of 1, 6 and $12 \text{ g cm}^{-2} \text{ h}^{-1}$ (Newton 1978²³) and FAR 25-C curves for 0, -10 and -20°C are shown for comparison.

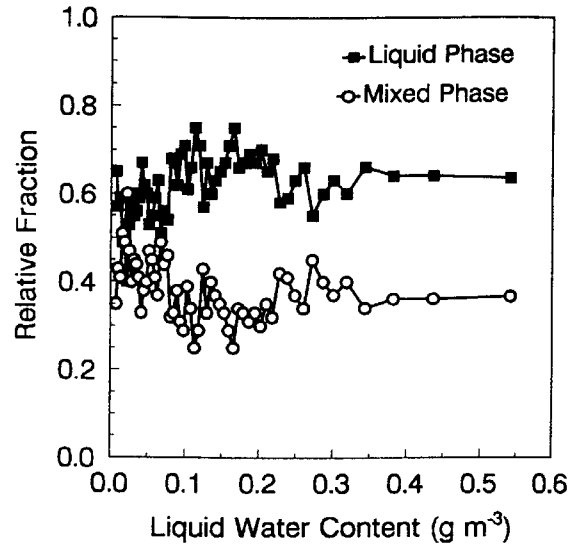


Figure 11. Plot of the relative frequencies of liquid and mixed-phase conditions as a function of LWC. The data were segregated by LWC into bins of 100 data points. For each bin the frequencies of liquid and mixed-phase conditions were determined. Each LWC data point represents the average LWC for that bin.

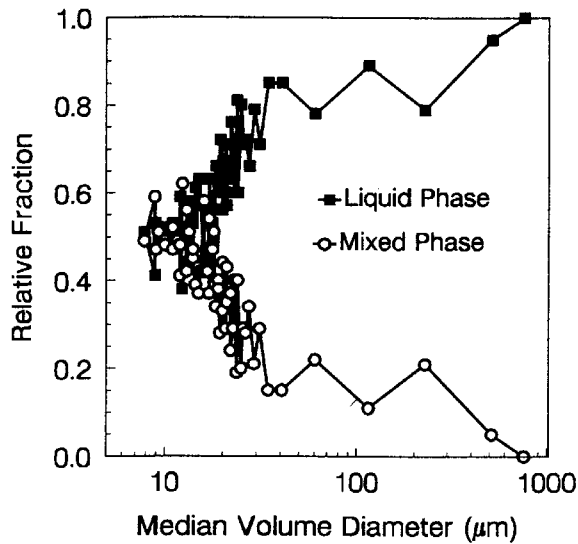


Figure 10. Plot of the relative frequencies of liquid and mixed-phase conditions as a function of the drop spectra MVD. The analysis is based on 5652 liquid and mixed-phase data points with ice crystal concentrations $< 1 \text{ L}^{-1}$. The data were segregated by MVD into bins of 100 data points. For each bin, the frequencies of liquid and mixed-phase conditions were determined. Each MVD data point represents the average MVD for that bin.